Noname manuscript No.
(will be inserted by the editor)

Efficient computation of Lyapunov functions for nonlinear systems by integrating numerical solutions

Sigurdur Freyr Hafstein · Asgeir Valfells

Received: date / Accepted: date

Abstract A strict Lyapunov function for an equilibrium of a dynamical system asserts its asymptotic stability and gives a lower bound on its basin of attraction. For nonlinear systems the explicit construction of a Lyapunov function taking the nonlinear dynamics into account remains a difficult problem and one often resorts to numerical methods. We improve and analyze a method that is based on a converse theorem in the Lyapunov stability theory and compare it to different methods in the literature. Our method is of low complexity and its workload is perfectly parallel. Further, its free parameters allow it to be adapted to the problem at hand and we show that our method matches or gives a larger lower bound on the equilibrium's basin of attraction than other approaches in the literature in most examples. Finally, we apply our method to a model of a genetic toggle switch in Escherichia coli and we demonstrate that our novel method delivers important information on the model's dynamics for different parameters.

Keywords Nonlinear system · Lyapunov function · Basin of attraction · Numerical method

1 Introduction

We consider the autonomous dynamical system,

$$\mathbf{x}' = \mathbf{f}(\mathbf{x}), \tag{1}$$

where $\mathbf{f}:\mathbb{R}^n \to \mathbb{R}^n$ is locally Lipschitz. We denote the unique solution to (1) with initial value $\xi \in \mathbb{R}^n$ at $t = 0$ with $t \mapsto \phi(t,\xi)$. If $\eta \in \mathbb{R}^n$ is an equilibrium point for (1), i.e. $\phi(t,\eta) = \eta$ a constant solution, its stability properties are of much practical interest. The equilibrium point η is said to be *stable* (in the sense of Lyapunov) if for every $\varepsilon > 0$ there exists a $\delta > 0$ such that $\|\xi - \eta\| < \delta$ implies $\|\phi(t,\xi) - \eta\| < \varepsilon$ for all $t \geq 0$. Here and elsewhere in the paper $\|\cdot\|$ denotes the Euclidian norm. The equilibrium is said to be *asymptotically stable* if it is stable and solutions started in a vicinity of the equilibrium are attracted to it. Then the open set

$$\mathscr{D}_\eta := \{\xi \in \mathbb{R}^n : \lim_{t\to\infty} \|\phi(t,\xi) - \eta\| = 0\}$$

is called the equilibrium's *basin of attraction*. Without loss of generality we may assume the equilibrium η of interest is at the origin, i.e. $\eta = 0$, and we will do so in this paper with the exception of our study of a genetic toggle switch in Section 4.

Stability of equilibrium points and basins of attraction are concepts of fundamental relevance in applications of dynamical systems and they are usually dealt with using the Lyapunov stability theory. Some good references are [18, 22, 24]. The centerpiece of the Lyapunov stability theory is the so-called Lyapunov function, a scalar-valued function from the state-space of the dynamical system that is decreasing along all solutions of the system in a neighbourhood of the equilibrium in question. Lyapunov functions deliver lower bounds on basins of attraction through their sublevel sets. For linear systems $\mathbf{x}' = A\mathbf{x}$ they can be constructed explicitly by solving the so-called Lyapunov equation $A^T P + AP = -Q$ for $P \in \mathbb{R}^{n\times n}$, where $Q \in \mathbb{R}^{n\times n}$ is a given symmetric and positive definite matrix. The positive definite function $V(\mathbf{x}) = \mathbf{x}^T P\mathbf{x}$ is then a global Lyapunov function for the system. For nonlinear systems there is no general method, but one can resort to linearization around the equilibrium in question and construct a Lyapunov function for the linearization. This Lyapunov function is also a Lyapunov function for the nonlinear system in a neighbourhood of the equilibrium, but it is not a good Lyapunov func-

S. Hafstein (corresponding author) orcid: 0000-0003-0073-2765 · A. Valfells
Faculty of Physical Sciences
University of Iceland
Dunhagi 5, 107 Reykjavik, Iceland
Hafstein tel. +354-6966325
E-mail: shafstein@hi.is, avalfells@gmail.com

tion in the sense that it does in general deliver very conservative lower bounds on the equilibrium's basin of attraction. For exact formulas see, e.g. [14].

2 Lyapunov Function Computation

For the reasons discussed in the last section there have been numerous methods proposed in the literature to generate Lyapunov functions for nonlinear systems [12]. One approach is to approximate numerically formulas for Lyapunov functions [1,15,5,6] from classical converse theorems [20,26, 17] in the Lyapunov stability theory. These converse theorems assert the existence of Lyapunov functions for systems with asymptotically stable equilibria and give formulas, in terms of the systems's solution, for these Lyapunov functions. Because these formulas include the solutions to the systems, that are in general not obtainable for nonlinear systems, one resorts to approximate their values at a finite number of points. The Lyapunov function must be decreasing along solution trajectories in a whole neighbourhood of the equilibrium in question. If this cannot be asserted the constructed (Lyapunov) function is of little use, i.e. an approximation to a Lyapunov function is of little value. Therefore the computed values must be interpolated such that the resulting function is a Lyapunov function in a whole area. This can be achieved by using the linear programming (LP) problem from [10], but instead of using LP to compute the values of the Lyapunov function at the vertices of a simplicial complex, one uses a formula from a converse theorem to assign values at the vertices and then verifies if the linear constraints of the LP problem are fulfilled using these values. If the linear constraints are fulfilled for all vertices of a certain simplex, then the affine interpolation of these values over the simplex defines a function, whose orbital derivative is negative along all solution trajectories passing through this simplex. This was already shown in [1].

To construct the LP problem the set $\mathscr{D} \subset \mathbb{R}^n$ that is to serve as the domain of the Lyapunov function to be computed is first subdivided into simplices. More exactly, the set $\mathscr{D}$ must be the union of n-simplices

$$\mathfrak{S}_\nu = \operatorname{co}\{\mathbf{x}_0^\nu, \mathbf{x}_1^\nu, \dots, \mathbf{x}_n^\nu\}, \quad \nu = 1:N,$$

where we abbreviate $1,2,\dots,N$ by $1:N$ and $\operatorname{co}\{\cdot\}$ stands for the *convex hull*, i.e. $\mathbf{x} \in \operatorname{co}\{\mathbf{x}_0^\nu, \mathbf{x}_1^\nu, \dots, \mathbf{x}_n^\nu\}$ if and only if

$$\mathbf{x} = \sum_{i=0}^{n} \lambda_i \mathbf{x}_i^\nu \text{ for some } \lambda_i \geq 0 \text{ such that } \sum_{i=0}^{n} \lambda_i = 1.$$

The vectors $\mathbf{x}_0^\nu, \mathbf{x}_1^\nu, \dots, \mathbf{x}_n^\nu$ are said to be the vertices of the simplex $\mathfrak{S}_\nu$. That $\mathfrak{S}_\nu$ is an n-simplex, i.e. has nonzero n-dimensional volume, is equivalent to its vertices $\mathbf{x}_0^\nu, \mathbf{x}_1^\nu, \dots, \mathbf{x}_n^\nu$ being affinely independent, which in turn is equivalent to the vectors $\mathbf{x}_1^\nu - \mathbf{x}_0^\nu, \mathbf{x}_2^\nu - \mathbf{x}_0^\nu, \dots, \mathbf{x}_n^\nu - \mathbf{x}_0^\nu$ being linearly independent. We write $\mathscr{T}$ for the collection of the simplices $\mathfrak{S}_\nu$, $\nu = 1:N$, and refer to it as the *triangulation*. We denote the set of all vertices of simplices in $\mathscr{T}$ by $\mathscr{V}_\mathscr{T}$. The equilibrium of interest, i.e. the origin, should be in $\mathscr{V}_\mathscr{T}$. The triangulation $\mathscr{T}$ must be *shape regular*, i.e. it must be a *simplicial complex*. This means that two different simplices $\mathfrak{S}_\nu, \mathfrak{S}_\mu \in \mathscr{T}$ are either disjoint or intersect in a common face, i.e. $\mathfrak{S}_\nu \cap \mathfrak{S}_\mu \neq \emptyset$ implies

$$\mathfrak{S}_\nu \cap \mathfrak{S}_\mu = \operatorname{co}\{\mathbf{y}_0, \mathbf{y}_1 \dots, \mathbf{y}_r\},$$

where $0 \leq r < n$ and the vectors $\mathbf{y}_0, \mathbf{y}_1 \dots, \mathbf{y}_r$ are vertices of $\mathfrak{S}_\nu$ and vertices of $\mathfrak{S}_\mu$.

The variables of the LP problem for system (1) are $V[\mathbf{x}] \in \mathbb{R}$ for all $\mathbf{x} \in \mathscr{V}_\mathscr{T}$. The linear constraints of the LP problem are constructed in such a way that the function $V : \mathscr{D} \to \mathbb{R}_+$ defined through

$$V(\mathbf{x}) = \sum_{i=0}^{n} \lambda_i V[\mathbf{x}_i^\nu], \text{ where } \mathbf{x} = \sum_{i=0}^{n} \lambda_i \mathbf{x}_i^\nu \in \mathfrak{S}_\nu, \tag{2}$$

is a Lyapunov function for the system. The linear constraints

$$V[0] = 0 \text{ and } V[\mathbf{x}] > 0 \text{ for all } \mathbf{x} \in \mathscr{V}_\mathscr{T} \setminus \{0\},$$

imply that the function has a minimum at the equilibrium at the origin. The second set of linear constraints in the LP problem are: for every $\mathfrak{S}_\nu \in \mathscr{T}$ and every vertex $\mathbf{x}_i^\nu$ of $\mathfrak{S}_\nu$ we demand

$$0 > \nabla V_\nu \cdot \mathbf{f}(\mathbf{x}_i^\nu) + E_\nu \|\nabla V_\nu\|_1. \tag{3}$$

Here ∇V_ν is the gradient of the function V on the interior of $\mathfrak{S}_\nu$, which is linear in its values at the vertices $V(\mathbf{x}_j^\nu) = V[\mathbf{x}_j^\nu]$, i.e. the variables of the LP problem, $\|\cdot\|_1$ is the norm $\|\mathbf{x}\|_1 := \sum_{j=1}^n |x_j|$, and E_ν is a system- and simplex dependant positive constant chosen such that V is guarantied to be decreasing along solution trajectories. If the LP problem has a feasible solution, i.e. there exist values for the variables $V[\mathbf{x}]$ such that all the constraints are fulfilled, then V defined by (2) is indeed a Lyapunov function for the system. For a detailed discussion on this LP problem cf. e.g. [10,11].

In a recent publication [16] the authors showed that for certain regular triangulations the constraints (3) can be written in a particularly efficient form for fast verification of the constraints and with less conservative bounds on the constants E_ν than in [10,11]. The main idea of this more efficient form is to use simplices whose sides are parallel to the axis, which implies that the gradient of V can be computed faster from the values of V at the vertices and that formula (4) for E_ν can be used, which gives lower values than the formulas used in [10,11].

Let us describe the triangulation: Denote by Sym_n the set of the permutations of $\{1:n\}$, by $\mathfrak{P}(\{1:n\})$ the powerset of $\{1:n\}$, and set $\mathscr{Z} := \mathbb{N}_0^n \times \mathfrak{P}(\{1:n\})$. Let PS_i, $i = 1:n$, be

strictly increasing functions $\mathbb{R}\to\mathbb{R}$ that vanish at zero and define $\mathbf{PS}:\mathbb{R}^n\to\mathbb{R}^n$, $\mathbf{PS}=(\mathrm{PS}_1,\mathrm{PS}_1,\dots,\mathrm{PS}_\mathrm{n})^T$. Define

$$\mathbf{R}^{\mathscr{J}}(\mathbf{x})=\sum_{i=1}^{n}(-1)^{\chi_{\mathscr{J}}(i)}x_i\mathbf{e}_i$$

for every $\mathscr{J}\in\mathfrak{P}(\{1:n\})$, where $\chi_{\mathscr{J}}$ is the characteristic function of the set $\mathscr{J}$, and

$$\mathbf{x}_i^{\mathbf{z}\mathscr{J}\sigma}:=\mathbf{R}^{\mathscr{J}}\left(\mathbf{z}+\sum_{j=1}^{i}\mathbf{e}_{\sigma(j)}\right)$$

for every $\sigma\in\mathrm{Sym}_n$, $i=0:n$, and $\mathscr{J}\in\mathfrak{P}(\{1:n\})$. Assume that $\mathbf{f}$ in the system (1) is C^2 and let $B_{rs}^{(\mathbf{z},\mathscr{J})}$ for every $(\mathbf{z},\mathscr{J})\in\mathscr{Z}$ and $r,s=1:n$ be a constant fulfilling

$$B_{rs}^{(\mathbf{z},\mathscr{J})}\geq\max_{\substack{\mathbf{x}\in\mathbf{PS}(\mathbf{R}^{\mathscr{J}}(\mathbf{z}+[0,1]^n))\\ k=1:n}}\left|\frac{\partial^2 f_k(\mathbf{x})}{\partial x_r\partial x_s}\right|$$

For every $(\mathbf{z},\mathscr{J})\in\mathscr{Z}$, every $k,i=1:n$, and every $\sigma\in\mathrm{Sym}_n$, define

$$A_{k,i}^{\mathbf{z}\mathscr{J}\sigma}:=|\mathbf{e}_k\cdot(\mathbf{x}_i^{\mathbf{z}\mathscr{J}\sigma}-\mathbf{x}_0^{\mathbf{z}\mathscr{J}\sigma})|.$$

Then the constraints (3) can be written in the form

$$\begin{aligned}0>&\sum_{j=1}^{n}\frac{V[\mathbf{x}_j^{\mathbf{z}\mathscr{J}\sigma}]-V[\mathbf{x}_{j-1}^{\mathbf{z}\mathscr{J}\sigma}]}{\mathbf{e}_{\sigma(j)}\cdot(\mathbf{x}_j^{\mathbf{z}\mathscr{J}\sigma}-\mathbf{x}_{j-1}^{\mathbf{z}\mathscr{J}\sigma})}f_{\sigma(j)}(\mathbf{x}_i^{\mathbf{z}\mathscr{J}\sigma})\\&+E_{\mathbf{z}\mathscr{J}\sigma}\sum_{j=1}^{n}\left|\frac{V[\mathbf{x}_j^{\mathbf{z}\mathscr{J}\sigma}]-V[\mathbf{x}_{j-1}^{\mathbf{z}\mathscr{J}\sigma}]}{\mathbf{e}_{\sigma(j)}\cdot(\mathbf{x}_j^{\mathbf{z}\mathscr{J}\sigma}-\mathbf{x}_{j-1}^{\mathbf{z}\mathscr{J}\sigma})}\right|,\end{aligned}$$

where

$$E_{\mathbf{z}\mathscr{J}\sigma}=\frac{1}{2}\sum_{r,s=1}^{n}B_{rs}^{(\mathbf{z},\mathscr{J})}A_{r,i}^{\mathbf{z}\mathscr{J}\sigma}(A_{s,i}^{\mathbf{z}\mathscr{J}\sigma}+A_{s,n}^{\mathbf{z}\mathscr{J}\sigma}).\tag{4}$$

Remark: Notionally it is often more convenient to suppress the dependance on $\mathbf{z}\mathscr{J}\sigma$ and just refer to a simplex $\mathfrak{S}_\nu$ rather than $\mathfrak{S}_{\mathbf{z}\mathscr{J}\sigma}$. When using this simplified notation one then refers to B_{rs}^{ν} and not $B_{rs}^{(\mathbf{z},\mathscr{J})}$ for all simplices $\mathfrak{S}_\nu$ such that $\mathfrak{S}_\nu\subset\mathbf{PS}(\mathbf{R}^{\mathscr{J}}(\mathbf{z}+[0,1]^n))$, and it is not difficult to see that one can use different estimates B_{rs}^{ν} for the different $\mathfrak{S}_\nu\subset\mathbf{PS}(\mathbf{R}^{\mathscr{J}}(\mathbf{z}+[0,1]^n))$, although this hardly justifies the effort.

We now discuss how to assign values to the variables of the LP problem that can be expected to give a Lyapunov function that gives a good lower bound on the basin of attraction. From the integral formula from the converse theorem in [20] the obvious candidate is to use the Lyapunov function

$$W(\mathbf{x})=\int_0^T\|\phi(\tau,\mathbf{x})\|^2d\tau\tag{5}$$

and assign $V[\mathbf{x}]=W(\mathbf{x})$ in the LP problem. This will in principle work for large enough $T>0$ if the equilibrium at the origin is exponentially stable and this approach is followed in [1]. The choice of the Lyapunov function in (5) is due to it's intuitive accessibility and as such we are easily able to manipulate it without losing the Lyapunov properties. Now consider the time-reversed van der Pol oscillator:

$$\mathbf{x}'=\mathbf{f}(\mathbf{x})\ \text{ with }\ \mathbf{f}(x,y)=\begin{pmatrix}y\\-x-y(1-x^2)\end{pmatrix}.\tag{6}$$

It has an asymptotically stable equilibrium at the origin and the boundary of its basin of attraction is an unstable periodic orbit. In Figure 1 we see the maximum lower bound on the basin of attraction we can derive from the Lyapunov function from (5), when computing its values at grid points and interpolating over the triangles. For details on how this is done see Section 3. We note that there is a non-negligible area in which the approximated function has a negative orbital derivative but where, however, the values of the calculated Lyapunov function are higher than the values at the periodic orbit. This means that the lower bound on the basin of attraction we can derive from this Lyapunov function is unnecessarily conservative. We would like to ascertain that these points are within our lower bound on the basin of attraction and would therefore like a similar Lyapunov function to (5) that takes lower values at points significantly within the basin of attraction while maintaining similar values at points its boundary.

From the structure of (5) and after some experimenting we were able to discern that the following function is a promising candidate:

$$W(\mathbf{x})=\int_0^T\frac{\|\phi(\tau,\mathbf{x})\|^2}{\delta+\|\phi(\tau,\mathbf{x})\|^p}d\tau\tag{7}$$

This is the specific Lyapunov function we will discuss in this paper and we will use it to assign values to the variables of the LP problem and compare the results to different approaches in the literature.

Let us discuss the formula (7) in more detail and the heuristic of how to fix the parameters δ,T, and p for a particular system. Although any continuous and positive definite function of ϕ under the integral will in principle do the job, cf. e.g. [2], the formula (7) has returned significantly larger lower bounds on the basin of attraction than other functions we have examined. The parameters are fixed as follows: we start with a coarse grid where we compute the values of $W(\mathbf{x})$ using formula (5), or equivalently using formula (7) with $\delta=p=0$. $T>0$ must be chosen so large that solutions starting in the area covered by the grid at $t=0$ are close to the equilibrium at $t=T$. If the level-sets of W run into the boundary of the basin of attraction close to the equilibrium we choose a positive δ and increase p by 0.2 and compute the values of $W(\mathbf{x})$ again using the new parameters. We then repeatedly increase p by 0.2 until our lower bound on the basin of attraction does not become larger. Note that by this

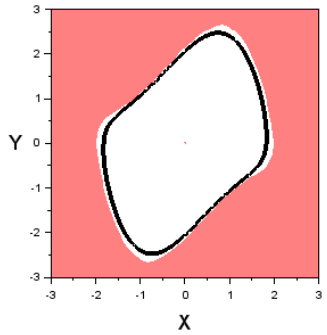

Fig. 1 A level-set of the Lyapunov function computed for the system (6) using formula (5) with $T = 20$. The area where the orbital derivative is not negative is drawn in red. Since the level-set does not intersect the area where the orbital derivative is nonnegative it is a lower bound on the basin of attraction of the equilibrium at the origin.

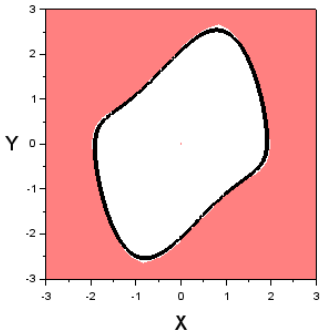

Fig. 2 A level-set of the Lyapunov function computed for the system (6) using formula (7) with $T = 20$, $\delta = 0.2$, and $p = 2$. The area where the orbital derivative is not negative is drawn in red. Since the level-set does not intersect the area where the orbital derivative is nonnegative it is a lower bound on the basin of attraction of the equilibrium at the origin.

procedure we push down the values of the integrand in formula (7) further away from the equilibrium. If the level-sets of W run into the boundary of the basin of attraction far from the equilibrium we similarly decrease the value of p in steps of 0.2. In this case we can use $\delta = 0$, because the integrand in (7) is a convex function of $\|\phi\|$. For $p > 0$ it is concave and not smooth at the equilibrium, and better results are obtained with $\delta > 0$.

3 Examples

We present four theoretical examples of our method and compare its results with different approaches in the literature. We approximate the Lyapunov function from (7) at the grid points with some appropriately chosen parameters T, δ, p. Then we interpolate and verify the negativity of the orbital derivative of the interpolation as in [1], but use the sharper error estimate (4) from [16] in the LP program. Note that the orbital derivative of the Lyapunov functions computed by our method is not guaranteed to be negative very close to the equilibrium. This is a known feature of the method and can be easily accounted for by using a local Lyapunov function for the linearized system at the equilibrium, which can be computed by the standard method of solving the Lyapunov equation. The points close to the equilibrium where the orbital derivative is not negative should be contained in a sublevel-set of a Lyapunov function for the linearized system and where it is also a Lyapunov function for the nonlinear system, because this sublevel-set is guaranteed to be in the basin of attraction. For explicit estimates of this area cf. e.g. [14, §4]. In all the examples presented this is a not an issue, because these points are very close to the equilibrium and can very easily be shown to be contained in such a sublevel-set of the Lyapunov function $V(\mathbf{x}) = \mathbf{x}^T P \mathbf{x}$, where P is the solution to the Lyapunov equation $A^T P + PA = -I$, A being the Jacobian of $\mathbf{f}$ at the equilibrium and I the identity matrix.

We compare our results with three other methods: the Massera construction from [1], i.e. where the Lyapunov function is approximated using (5) at the vertices; the approach from [23] as implemented and optimized in [21], where a rational Lyapunov function is computed, and the method presented in [4], where Lyapunov functions that are sums of squared polynomials (SOS) are computed with the program SMRSOFT [4]. Our method and the method from [1] were implemented in C++ and run on a PC with an i9-7900X processor. We used the Adams-Bashforth four-step method to numerically integrate the initial-value problems, taking the first three initial steps with the Runge-Kutta method of order four (RK4), and the numerical integrals were approximated using Simpson's rule. In all cases we used 1,000 steps, independent of T.

There are other methods to compute Lyapunov functions, see [12] for an overview, but we specifically choose the ones from [23,21,4] because they are computationally similarly demanding in our examples and are supposed to compute true Lyapunov functions and not approximations thereof. One should however note that in most of the examples SMRSOFT reported *(SMRSOFT message) SDP solving: SeDuMi numerical problems warning (numerr=1)"*, and we are not sure if the computed functions are true Lyapunov functions in all cases.

3.1 Example 1

The first example is a planar system from [9, Ex. 6],

$$\mathbf{x}' = \mathbf{f}(\mathbf{x}) \quad \text{with} \quad \mathbf{f}(x,y) = \begin{pmatrix} -x+y \\ 0.1x - 2y - x^2 - 0.1x^3 \end{pmatrix}. \tag{8}$$

We assign in the LP problem (notation from the Remark in the last section)

$$B^v_{1,1} = 2 + 0.6 \max_{(x,y)\in\mathfrak{S}_v} |x| \quad \text{and} \quad B^v_{1,2} = B^v_{2,1} = B^v_{2,2} = 0.$$

We set $T = 20$ for formulas (5) and (7) and for the latter we set $\delta = 0.6$, and $p = 1.2$. The grid used for the vertices of the simplices was 2001×2001 with 4,004,001 points and 8,000,000 simplices/triangles. This corresponds to using the simplices $\mathfrak{S}_{\mathbf{z}\mathscr{J}\sigma}$ for $\mathbf{z} \in \{0:999\}^2$, $\mathscr{J} \in \{\emptyset, \{1\}, \{2\}, \{1,2\}\}$, and $\sigma \in \{(1,2),(2,1)\}$ in the notation of Section 2. The computation of the Lyapunov function using formula (5) was done on the rectangle $[-20,20]^2$, i.e. the mapping **PS** from Section 2 is given by $\mathbf{PS}(\mathbf{x}) = 0.02\mathbf{x}$ (because $0.02 \cdot 1000 = 20$). The computation took 43.6 s and the verification of the negativity of the orbital derivative took 0.45 s. In 11.96% of the simplices/triangles the orbital derivative was not negative. For the computation using formula (7) on the rectangle $[-20,20] \times [-40,40]$, i.e. $\mathbf{PS}(x,y) = (0.02x, 0.04y)^T$, the corresponding run times were 51.8 s and 0.45 s. In 10.05% of the simplices/tirangles the orbital derivative was not negative. In figures 3 and 4 the Lyapunov functions using formulas (5) and (7) respectively are plotted. In figures 5 and 6 the level sets $\{\mathbf{x} \in \mathbb{R}^2 : V(\mathbf{x}) \le 33\}$ and $\{\mathbf{x} \in \mathbb{R}^2 : V(\mathbf{x}) \le 9\}$ for these functions are plotted. These level sets are chosen, using trial and error, such that they do not intersect with the areas where the orbital derivative is nonnegative and thus give lower bounds on the basin of attraction.

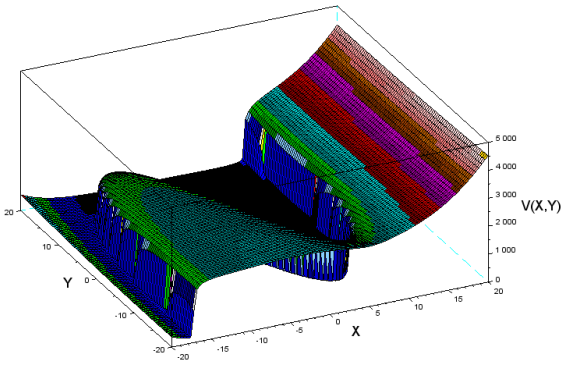

Fig. 3 The Lyapunov function computed for system (8) using formula (5).

In Figure 7 we compare our results with the approaches from [23,21] and [4]. For the case using [4] we computed the 4th, 6th, and 8th order polynomial Lyapunov functions, but only draw the level-set for the 4th order one, because it delivered the least conservative estimate. It is notable, that even though this method delivers a significantly smaller lower bound on the basin of attraction than our method, it is not a proper subset of our bounds. Since the union of lower bounds on the basin of attraction is also a lower bound, it can be beneficial to use different method to obtain a superior lower bound.

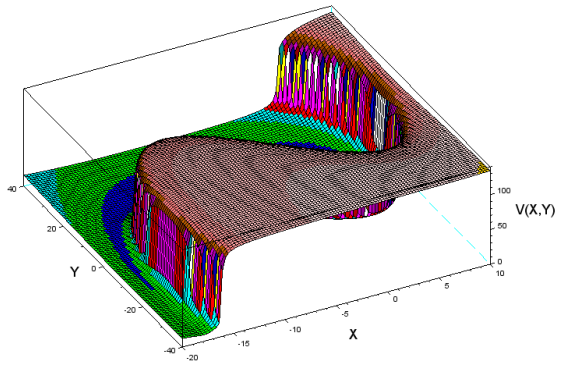

Fig. 4 The Lyapunov function computed for system (8) using formula (7) with $\delta = 0.6$ and $p = 1.2$.

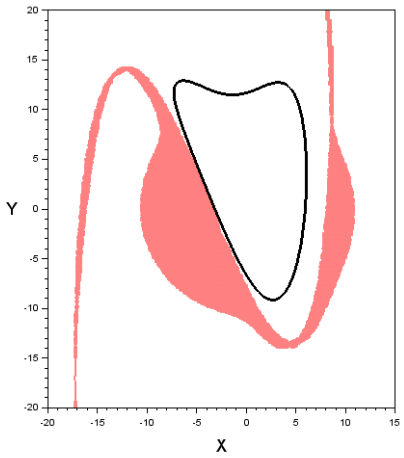

Fig. 5 A level-set of the Lyapunov function computed for the system (8) using formula (5). The area where the orbital derivative is not negative is drawn in red. Since the level-set does not intersect the area where the orbital derivative is nonnegative it is a lower bound on the basin of attraction of the equilibrium at the origin.

3.2 Example 2

The second example is a planar system from [25],

$$\mathbf{x}' = \mathbf{f}(\mathbf{x}) \quad \text{with} \quad \mathbf{f}(x,y) = \begin{pmatrix} -0.84x - 1.44y - 0.3xy \\ 0.54x + 0.34y + 0.3xy \end{pmatrix}. \tag{9}$$

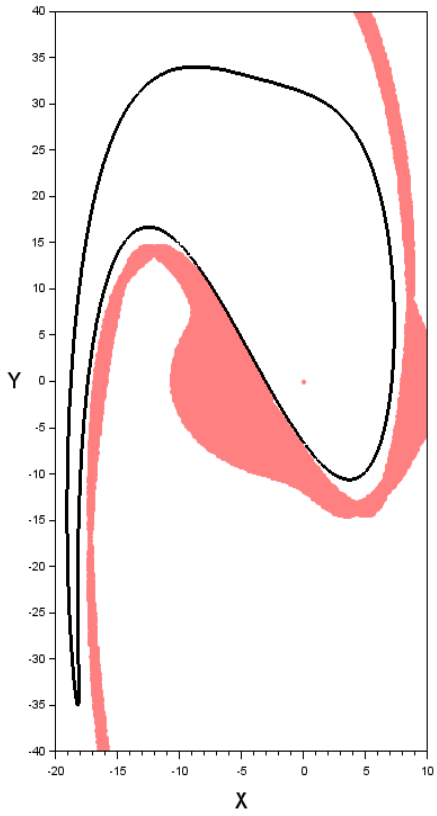

Fig. 6 A level-set of the Lyapunov function computed for the system (8) using formula (7) with $\delta = 0.6$ and $p = 1.2$. The area where the orbital derivative is not negative is drawn in red. Since the level-set does not intersect the area where the orbital derivative is nonnegative it is a lower bound on the basin of attraction of the equilibrium at the origin. Note that the lower bound on the basin of attraction is much larger than given by the Lyapunov function computed using formula (5).

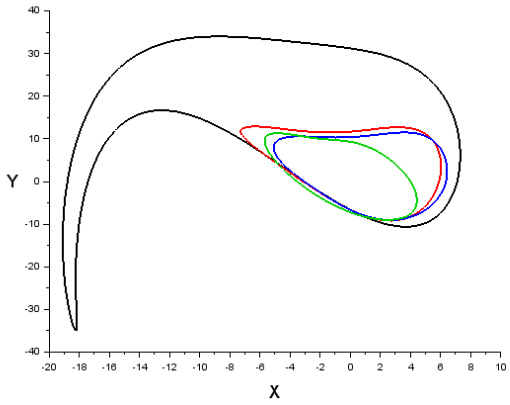

Fig. 7 Level-sets of the Lyapunov functions computed for the system (8) using formula (7) (outermost, black), formula (5) (red), the method from [23,21] (blue), and using the software SMRSOFT [4] (green).

We assign

$$B^V_{1,2} = B^V_{2,1} = 0.3 \quad \text{and} \quad B^V_{1,1} = B^V_{2,2} = 0.$$

We set $T = 20$ in formulas (5) and (7) and for the latter we set $\delta = 0.3$ and $p = 1.4$. The grid used for the vertices of the simplices was 2001×2001 with 4,004,001 points and 8,000,000 simplices/triangles. The computation of the Lyapunov function using formula (5) was done on the rectangle $[-8,8] \times [-2,8]$ and took 37 s and the verification of the negativity of the orbital derivative took 0.47 s. In 24.69% of the simplices/triangles the orbital derivative was not negative. In most of the area where the orbital derivative was not negative the Lyapunov function was not defined because the initial-value problems diverge too fast on the interval $[0,T]$ for the numerical solver.

For the computation using formula (7) on the same rectangle and with the same grid the corresponding run time numbers were 49.5 s and 0.49 s. In 24.71% of the simplices/triangles the orbital derivative was not negative. Again, mostly due to the numerical solver being unable to assign values to the Lyapunov function at the grid points.

In figures 8 and 9 the Lyapunov functions using formulas (5) and (7) respectively are plotted. In figures 10 and 11 the level sets $\{\mathbf{x} \in \mathbb{R}^2 : V(\mathbf{x}) \leq 10\}$ and $\{\mathbf{x} \in \mathbb{R}^2 : V(\mathbf{x}) \leq 9\}$ for these functions are plotted. These level sets are chosen such that they do not intersect with the areas where the orbital derivative is nonnegative and thus give lower bounds on the basin of attraction.

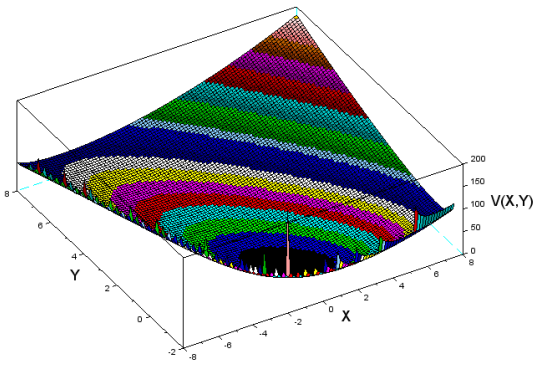

Fig. 8 The Lyapunov function computed for system (9) using formula (5).

In Figure 12 we compare our results with the approach from [23,21]. We omit the method from [4] since when system (9) is entered into SMRSOFT the program returns an error and is not able to solve the semidefinite optimization problem.

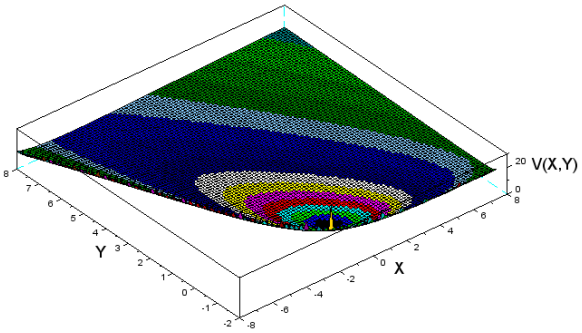

Fig. 9 The Lyapunov function computed for system (9) using formula (7) with $\delta = 0.3$ and $p = 1.4$.

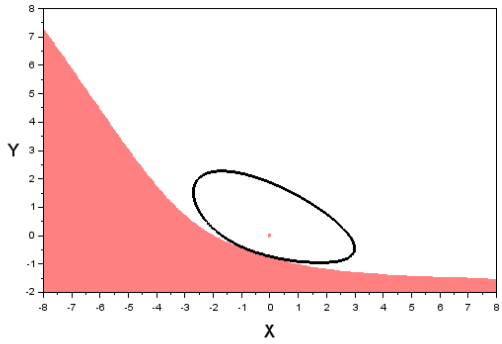

Fig. 10 A level-set of the Lyapunov function computed for the system (9) using formula (5). The area where the orbital derivative is not negative is drawn in red. Since the level-set does not intersect the area where the orbital derivative is nonnegative it is a lower bound on the basin of attraction of the equilibrium at the origin.

3.3 Example 3

The third example is a nonpolynomial planar system from [3, Ex. 1],

$$\mathbf{x}' = \mathbf{f}(\mathbf{x}) \text{ with } \mathbf{f}(x,y) = \begin{pmatrix} -x+y+\frac{1}{2}(e^x-1) \\ -x-y+xy+x\cos(x) \end{pmatrix}. \quad (10)$$

We assign

$$B^v_{1,1} = \max_{(x,y)\in\mathfrak{S}_v} \max(e^x/2, 2|\sin(x)| + |x\cos(x)|),$$
$$B^v_{1,2} = B^v_{2,1} = 1, \text{ and } B^v_{2,2} = 0.$$

Further, we set $T = 20$ for formulas (5) and (7) and for latter we set $\delta = 0.4$, and $p = 0.6$. As in examples 1 and 2 the grid was 2001×2001 with 4,004,001 points and 8,000,000 simplices/triangles. The computation of the Lyapunov function using formula (5) was done on the rectangle $[-8,4] \times [-8,8]$ and took 35.6 s and the verification of the negativity of the orbital derivative took 0.4 s. In 27.9% of the simplices/triangles the orbital derivative was not negative. In most of the area where the orbital derivative was not negative the Lyapunov function was not even defined because the initial-value problems diverge too fast on the interval $[0,T]$ for the numerical solver. Note that if the Lyapunov function is not defined at one or more vertices of a simplex, then it is not properly defined on that simplex neither is its orbital derivative. In particular, its orbital derivative cannot be negative.

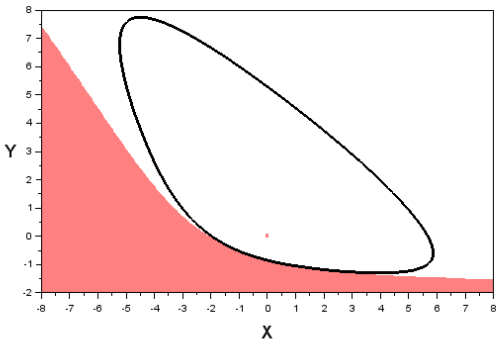

Fig. 11 A level-set of the Lyapunov function computed for the system (9) using formula (7) with $\delta = 0.3$ and $p = 1.4$. The area where the orbital derivative is not negative is drawn in red. Since the level-set does not intersect the area where the orbital derivative is nonnegative it is a lower bound on the basin of attraction of the equilibrium at the origin. Note that the lower bound on the basin of attraction is much larger than given by the Lyapunov function computed using formula (5).

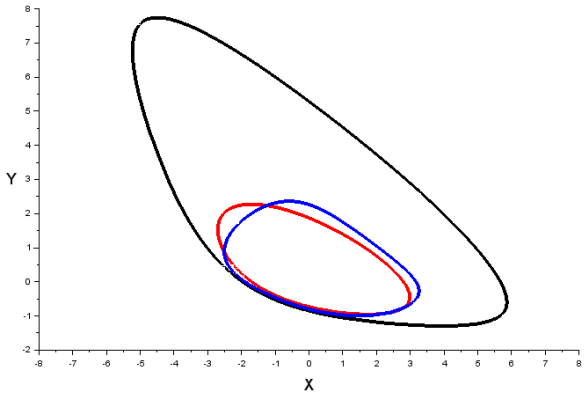

Fig. 12 Level-sets of the Lyapunov functions computed for the system (9) using formula (7) (outermost, black), formula (5) (red), and the method from [23,21] (blue).

For the computation using formula (7) on the rectangle $[-8,3] \times [-10,10]$ the corresponding numbers were 45.2 s and 0.4 s. In 23.4% of the simplices/triangles the orbital deriva-

tive was not negative, also mostly because the numerical solver was not able to assign values to the Lyapunov function at the grid points.

In figures 13 and 14 the Lyapunov functions using formulas (5) and (7) respectively are plotted. In figures 15 and 16 the level sets $\{\mathbf{x}\in\mathbb{R}^2 : V(\mathbf{x})\le 8\}$ and $\{\mathbf{x}\in\mathbb{R}^2 : V(\mathbf{x})\le 5.9\}$ for these functions are plotted. These level sets are chosen such that they do not intersect with the ares where the orbital derivative is nonnegative and thus give lower bounds on the basin of attraction.

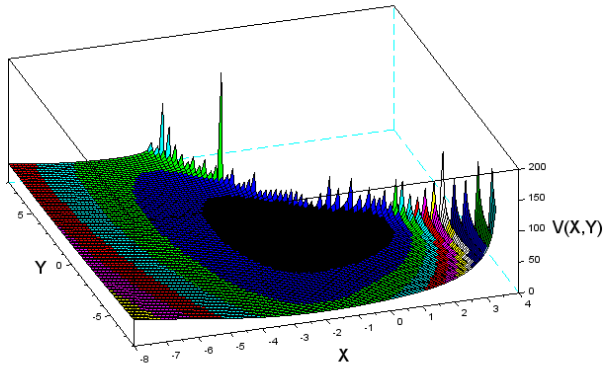

Fig. 13 The Lyapunov function computed for system (10) using formula (5).

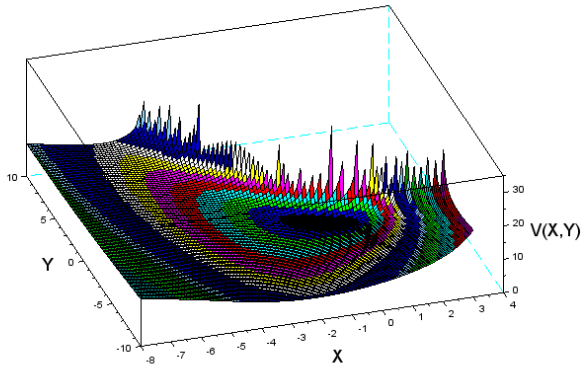

Fig. 14 The Lyapunov function computed for system (10) using formula (7) with $\delta = 0.4$ and $p = 0.6$.

In Figure 17 we compare our results with the approach from [23] as implemented in [21], where a rational Lyapunov function is computed for the same system. We also compared it with the method from [3], but the level sets obtained are very close to the ones from [21] and we therefore omit drawing them.

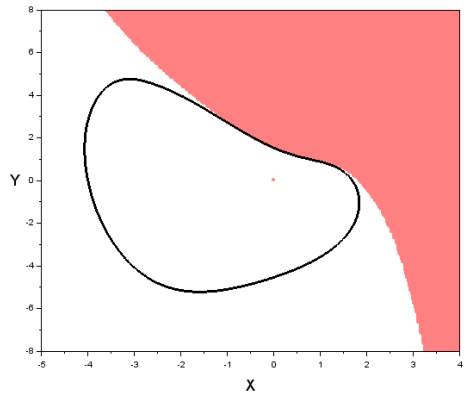

Fig. 15 Level-sets of the Lyapunov function computed for the system (10) using formula (5). The area where the orbital derivative is not negative is drawn in red. Since the level-set does not intersect the area where the orbital derivative is nonnegative it is a lower bounds on the basin of attraction of the equilibrium at the origin.

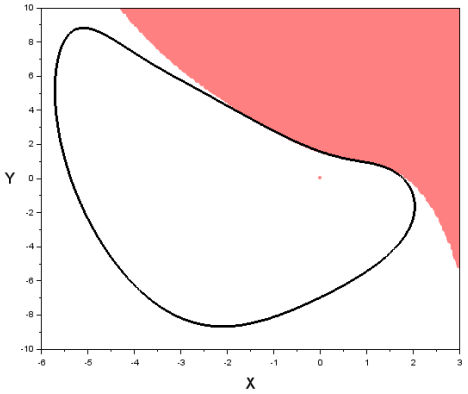

Fig. 16 Level-sets of the Lyapunov function computed for the system (10) using formula (7) with $\delta = 0.4$ and $p = 0.6$. The area where the orbital derivative is not negative is drawn in red. Since the level-set does not intersect the area where the orbital derivative is nonnegative it is a lower bound on the basin of attraction of the equilibrium at the origin.

3.4 Example 4

The fourth example is a three-dimensional system from [13], also studied in [21]:

$$\mathbf{x}' = \mathbf{f}(\mathbf{x}) \quad \text{with} \quad \mathbf{f}(x,y,z) = \begin{pmatrix} -x+y+z^2 \\ -y+xy \\ -z \end{pmatrix}. \tag{11}$$

We assign

$$B^V_{1,2} = B^V_{2,1} = 1,\ B^V_{3,3} = 2,\ \text{and}\ B^V_{r,s} = 0 \ \text{ in all other cases.}$$

Further, we set $T = 10$ in formulas (5) and (7) and for latter we set $\delta = 1$ and $p = 2$. The grid was $201\times 201\times 101$

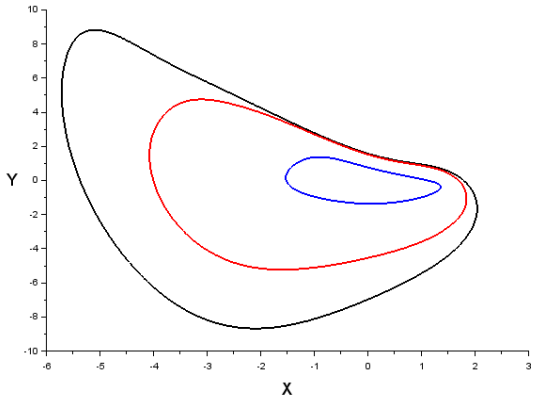

Fig. 17 Level-sets of the Lyapunov functions computed for the system (10) using formula (7) (outermost, black), (5) (middle, red), and by using the method from [23,21] (innermost, blue). In [3] results very close to the ones from [23,21] are obtained using SOS programming.

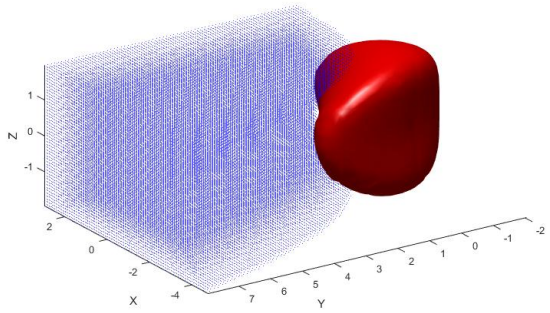

Fig. 18 Level-set of the Lyapunov function computed for the system (11) using formula (5). The area where the orbital derivative is not negative is drawn in blue. Since the level-set does not intersect the area where the orbital derivative is nonnegative it is a lower bound on the basin of attraction of the equilibrium at the origin.

with $4,080,501$ points and 24,000,000 simplices/tetrahedra. The computation of the Lyapunov function using formula (5) was done on the cube $[-8,3]\times[-3,8]\times[-2,2]$ and took 40.7 s and the verification of the negativity of the orbital derivative took 1.5 s. In 32.4% of the simplices/tetrahedra the orbital derivative was not negative. In most of the area where the orbital derivative was not negative the Lyapunov function was not defined because the initial-value problems diverge too fast on the interval $[0,T]$ for the numerical solver.

For the computation using formula (7) on the same cube and using the same grid the corresponding run times were 40.6 s and 1.85 s. In 36.1% of the simplices/tetrahedra the orbital derivative was not negative, also mostly because the numerical solver was not able to assign values to the Lyapunov function at the grid points.

In figures 18 and 19 the level-sets $\{\mathbf{x}\in\mathbb{R}^3 : V(\mathbf{x})\leq 2.2\}$ and $\{\mathbf{x}\in\mathbb{R}^3 : V(\mathbf{x})\leq 0.85\}$ for the Lyapunov functions using formulas (5) and (7) respectively are plotted. These level sets are chosen such that they do not intersect with the ares where the orbital derivative is nonnegative and thus give lower bounds on the basin of attraction.

Note that the level-sets for the Lyapunov functions in figures 18 and 19 are very different. For the Lyapunov function constructed using formula (5) it is thicker and the level-set of the Lyapunov function constructed using formula (7) is thinner and extends along the separatrix.

We did another experiment using formula (7), still with $T=10$, but now with $\delta=0.5$ and $p=1$ and using the grid $151\times151\times151$ and the cube $[-8,3]\times[-3,8]\times[-3,3]$. This corresponds to $3,442,951$ grid points and 20,250,000 simplices/tetrahedra. The run time for the computation of the Lyapunov function was 43.8 s and the verification of the negativity of the orbital derivative took 1.2 s. In 38.1% of the simplices/tetrahedra the orbital derivative was not negative. In most of the area where the orbital derivative was not negative the Lyapunov function was not defined because the initial-value problems diverge too fast on the interval $[0,T]$ for the numerical solver.

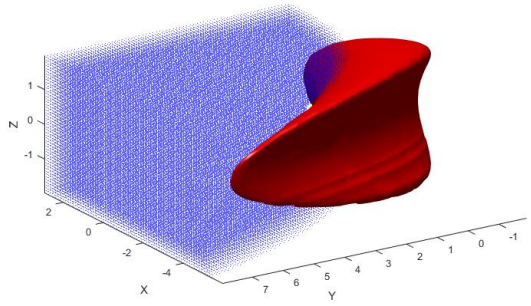

Fig. 19 Level-set of the Lyapunov function computed for the system (11) using formula (7) with $\delta=1$ and $p=2$. The area where the orbital derivative is not negative is drawn in blue. Since the level-set does not intersect the area where the orbital derivative is nonnegative it is a lower bound on the basin of attraction of the equilibrium at the origin.

In Figure 20 the level-set $\{\mathbf{x}\in\mathbb{R}^3 : V(\mathbf{x})\leq 1.3\}$ is plotted for this Lyapunov function, chosen such that it does not intersect with the area where the orbital derivative fails to be negative. This level-set resembles the one for the Lyapunov function computed using formula (5), cf. Figure 18, more than the one computed using formula (7) with $\delta=1$ and $p=2$, cf. Figure 19. However, it extends further in the z-direction.

We compared our approach with results from [23,21], where a rational Lyapunov function is computed for the same

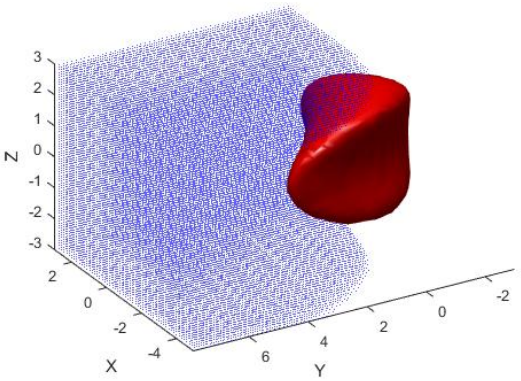

Fig. 20 Level-set of the Lyapunov functions computed for the system (11) using formula (7) with $\delta = 0.5$ and $p = 1$. The area where the orbital derivative is not negative is drawn in blue. Since the level-set does not intersect the area where the orbital derivative is nonnegative it is a lower bound on the basin of attraction of the equilibrium at the origin.

system, and [3] where SOS programming is used. In Figure 21 the sublevel-set $\{\mathbf{x} \in \mathbb{R}^3 : V(\mathbf{x}) \leq 1.32\}$ for the Lyapunov function computed in [21, E5] is plotted. The ranges of the axes is the same as in figures 18 and 19. Note that the sublevel-set is not connected, but the connected component containing the origin is a lower bound on the basin of attraction of the equilibrium at the origin.

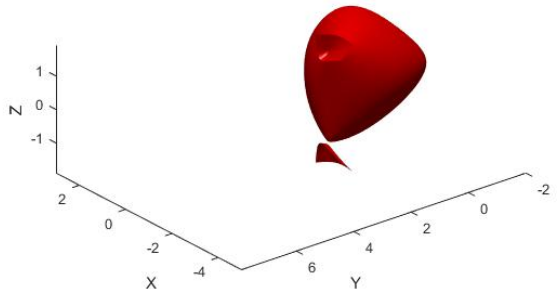

Fig. 21 Level-set of the Lyapunov function computed for the system (11) using the approach from [21]. The formula for the function is given in Table 2 E5 in that paper. The connected component of the sublevel-set containing the origin is a lower bound on the basin of attraction of the equilibrium at the origin.

In Figure 22 the level-set $\{\mathbf{x} \in \mathbb{R}^3 : V(\mathbf{x}) = 1\}$ for the quadratic Lyapunov function computed for system (11) using SMRSOFT [3] is plotted. The ranges of the axes is the same as in figures 18, 19, and 21.

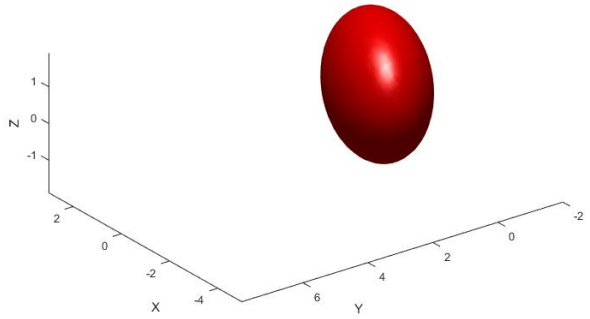

Fig. 22 Level-set of the quadratic Lyapunov function computed for the system (11) using SMRSOFT [3]. The area where the orbital derivative is not negative is drawn in red. The sublevel-set is a lower bound on the basin of attraction of the equilibrium at the origin.

In Figure 23 the level-set $\{\mathbf{x} \in \mathbb{R}^3 : V(\mathbf{x}) = 1\}$ for the fourth-order polynomial Lyapunov function computed for system (11) using SMRSOFT [3] is plotted. The ranges of the axes is the same as in Figure 20 (not the same as in figures 18, 19, and 21). The results are considerably better than from the quadratic Lyapunov function in Figure 22, but since the SeDuMi solver used for in the SOS programming reported a numerical error warning, we are not sure if the sublevel-set really is a rigid lower bound on the basin of attraction.

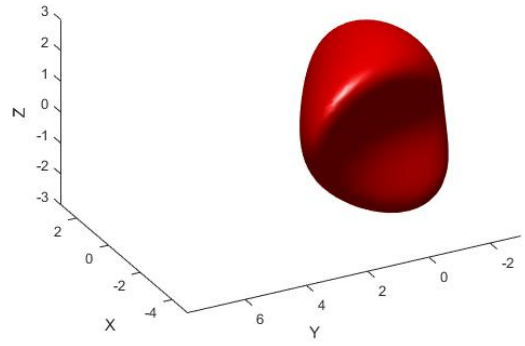

Fig. 23 Level-set of the fourth-order polynomial Lyapunov function computed for the system (11) using SMRSOFT [3]. The area where the orbital derivative is not negative is drawn in red. The sublevel-set is a lower bound on the basin of attraction of the equilibrium at the origin.

We also used SMRSOFT to compute a sixth-order polynomial Lyapunov function for system (11), but the results were not better that from the fourth-order one and SeDuMi

reported a numerical error warning and therefore we do not plot the results.

For system (11) our results are not as clearly superior to the ones from [23,21] and [3] as in the other examples, at least if the fourth-order polynomial

$$\begin{aligned}V(x,y,z) = {} & 0.1771x^2 + 0.2337xy + 0.0556xz + 0.2104y^2 \\ & + 0.02298yz + 0.04633z^2 - 0.001249x^3 \\ & + 0.06255x^2y - 0.008129x^2z + 0.1787xy^2 \\ & - 0.01053xyz + 0.1238xz^2 + 0.07677y^3 \\ & - 0.006475y^2z + 0.1222yz^2 + 0.01657z^3 \\ & + 0.001223x^4 + 0.002323x^3y - 0.001498x^3z \\ & + 0.01586x^2y^2 - 0.004996x^2yz + 0.005309x^2z^2 \\ & + 0.02875xy^3 - 0.01361xy^2z + 0.03808xyz^2 \\ & - 0.005758xz^3 + 0.0225y^4 - 0.01202y^3z \\ & + 0.05405y^2z^2 - 0.01403yz^3 + 0.03193z^4\end{aligned}$$

computed by SMRSOFT really is a Lyapunov function for the system (11). Note, however, that neither are the bounds we get subsets of the bounds from SMRSOFT nor vice-versa.

4 Case study: Genetic toggle switch

To demonstrate the applicability of our method we use it to study the dynamics of a model of a genetic toggle switch, i.e. a synthetic, bistable gene-regulatory network, presented in [8] and derived from a biochemical rate equation formulation of gene expression:

$$X' = \frac{\alpha_X}{1+Y^\beta} - X, \quad Y' = \frac{\alpha_Y}{1+X^\gamma} - Y \tag{12}$$

In this dimensionless model X and Y are variables and $\alpha_X, \alpha_Y, \beta$, and γ are constants with the following interpretation:

X is the concentration of repressor A,

Y is the concentration of repressor B,

α_X is the effective rate of synthesis of repressor A,

α_Y is the effective rate of synthesis of repressor B,

β is the cooperativity of repression of promoter B, and

γ is the cooperativity of repression of promoter A.

If $\beta, \gamma > 1$ the system (12) is bistable, i.e. has two stable equilibria. This model has been previously studied by numerical methods in [5,7] and recently the feedback control of such a system, keeping the system state for extended periods of time in the vicinity of a third unstable equilibrium, was studied both in the model and experimentally in [19]. The dynamics of this model has thus been demonstrated to be of importance in the field of cybergenetics, i.e. the novel field of remotely piloting cellular processes to leverage the biotechnical potential of synthetic biology.

First we analysed the model using the same parameters as in [5,7]: $\alpha_X = 1.3$, $\alpha_Y = 1$, $\beta = 3$, and $\gamma = 10$. We concentrate on the equilibrium point $\mathbf{z} = (0.66679013, 0.98292302)^T$, because it is more difficult to give a lower bound on its estimation of the basin of attraction than for the other stable equilibrium at $(1.29959444, 0.06782925)^T$. For an equilibrium at $\mathbf{z} \neq 0$ the formulas (5) and (7) must be modified to

$$W(\mathbf{x}) = \int_0^T \|\phi(\tau,\mathbf{x}) - \mathbf{z}\|^2 d\tau \tag{13}$$

and

$$W(\mathbf{x}) = \int_0^T \frac{\|\phi(\tau,\mathbf{x}) - \mathbf{z}\|^2}{\delta + \|\phi(\tau,\mathbf{x}) - \mathbf{z}\|^p} d\tau \tag{14}$$

respectively. In all the computations in this section we set $\delta = 0$, $T = 20$, and used the same 2001×2001 grid and 1,000 steps for the numerical integration as for the planar systems in Section 3. The running times of the computations for each example were all well below 1 minute and upper bounds for the parameters $B^V_{i,j}$ can be obtained in a straightforward way. Therefore we omit discussing these in detail.

In figures 24 and 25 the level-sets $\{\mathbf{x} \in \mathbb{R}^2 : V(\mathbf{x}) \leq 0.37\}$ and $\{\mathbf{x} \in \mathbb{R}^2 : V(\mathbf{x}) \leq 1.16\}$ for the Lyapunov functions using formulas (13) and (14) with $p = 0.8$ respectively are plotted. The lower bound on the basin of attraction using formula (13) is comparable to the results obtained in [5, 7] but the lower bounds gained from formula (14) are considerably larger, which demonstrates the power of our novel approach.

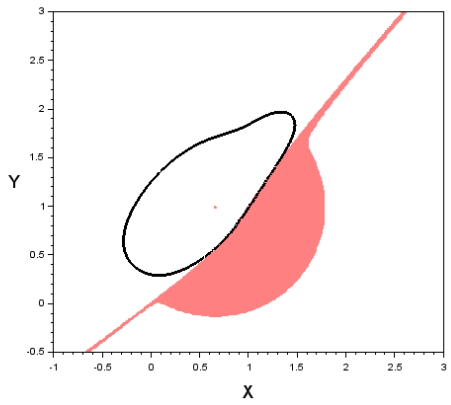

Fig. 24 Level-set of the Lyapunov function computed for the genetic toggle switch (12) with parameters $\alpha_X = 1.3$, $\alpha_Y = 1$, $\beta = 3$, and $\gamma = 10$ and using formula (13). The area where the orbital derivative is not negative is drawn in red. Since the level-set does not intersect the area where the orbital derivative is nonnegative it is a lower bound on the basin of attraction of the equilibrium at $\mathbf{z} = (0.66679013, 0.98292302)^T$.

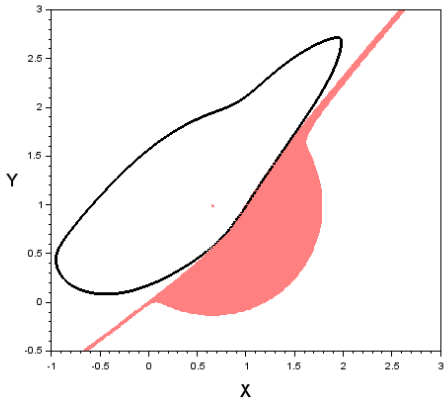

Fig. 25 Level-set of the Lyapunov function computed for the genetic toggle switch (12) with parameters $\alpha_X = 1.3$, $\alpha_Y = 1$, $\beta = 3$, and $\gamma = 10$ and using formula (14) with $\delta = 0$ and $p = 0.8$. The area where the orbital derivative is not negative is drawn in red. Since the level-set does not intersect the area where the orbital derivative is nonnegative it is a lower bound on the basin of attraction of the equilibrium at $\mathbf{z} = (0.66679013, 0.98292302)$.

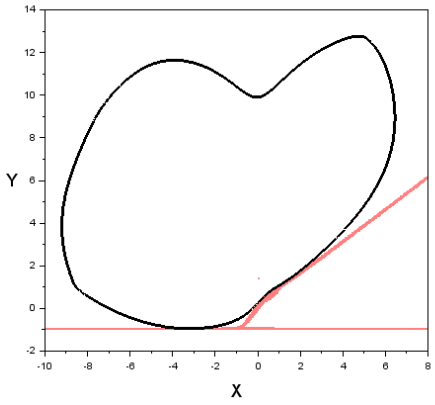

Fig. 27 Level-set of the Lyapunov function computed for the genetic toggle switch (12) with parameters $\alpha_X = 1$, $\alpha_Y = 1.4$, $\beta = 9$, and $\gamma = 2$ and using formula (14) with $\delta = 0$ and $p = 1.4$. The area where the orbital derivative is not negative is drawn in red. Since the level-set does not intersect the area where the orbital derivative is nonnegative it is a lower bound on the basin of attraction of the equilibrium at $\mathbf{z} = (0.04705013, 1.39690765)^T$.

We did numerical experiments with two other sets of parameters not reported in the literature. For the first experiment we set $\alpha_X = 1$, $\alpha_Y = 1.4$, $\beta = 9$, and $\gamma = 2$. With these parameters the toggle switch (12) has has stable equilibria at $\mathbf{z} = (0.04705013, 1.39690765)^T$ and $(0.92903424, 0.75143392)^T$. We consider the more difficult one $\mathbf{z}$. In figures 26 and 27 the level-sets $\{\mathbf{x} \in \mathbb{R}^2 : V(\mathbf{x}) \leq 6.3\}$ and $\{\mathbf{x} \in \mathbb{R}^2 : V(\mathbf{x}) \leq 6.16\}$ for the Lyapunov functions using formulas (13) and (14) with $p = 1.4$ respectively are plotted. The lower bounds using formula (14) are much larger (note the different scales on the axes) than those obtained using formula (13), which again demonstrates the power of our method.

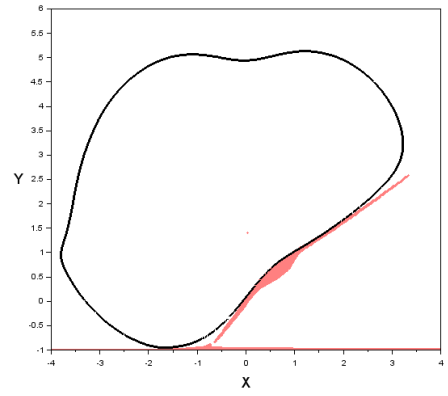

Fig. 26 Level-set of the Lyapunov function computed for the genetic toggle switch (12) with parameters $\alpha_X = 1$, $\alpha_Y = 1.4$, $\beta = 9$, and $\gamma = 2$ and using formula (13). The area where the orbital derivative is not negative is drawn in red. Since the level-set does not intersect the area where the orbital derivative is nonnegative it is a lower bound on the basin of attraction of the equilibrium at $\mathbf{z} = (0.04705013, 1.39690765)^T$.

For the final experiment we set $\alpha_X = 2$, $\alpha_Y = 4$, $\beta = 3$, and $\gamma = 5$. With these parameters the toggle switch (12) has has stable equilibria at $\mathbf{z} = (0.99634897, 0.12229057)^T$ and $(0.03076923, 3.99999989)^T$. As before we consider the more difficult one $\mathbf{z}$. In figures 28 and 29 the level-sets $\{\mathbf{x} \in \mathbb{R}^2 : V(\mathbf{x}) \leq 0.56\}$ and $\{\mathbf{x} \in \mathbb{R}^2 : V(\mathbf{x}) \leq 0.47\}$ for the Lyapunov functions using formulas (13) and (14) with $p = -0.8$ respectively are plotted. The lower bounds using formula (14) are somewhat larger than those obtained using formula (13), but does not entirely contain it. In this case a superior estimate is obtained by noting that the union of two rigid lower bounds on the basin of attraction is also a rigid lower bound on the basin of attraction, see Figure 30.

5 Conclusions

We presented a novel method to estimate the basin of attraction for asymptotically stable equilibria of dynamical systems. The method is based on approximating the values of Lyapunov functions from converse theorems and assign these values to the variables of a linear programming problem. The linear constraints of the problem are then verified and in simplices, of which they are fulfilled at all vertices, the function defined by interpolating these values over the simplex has a negative orbital derivative along the solutions of the system. Our method is an advancement of the method presented in [1], but with the sharper error estimates from [16] and thus less conservative linear constraints and a more

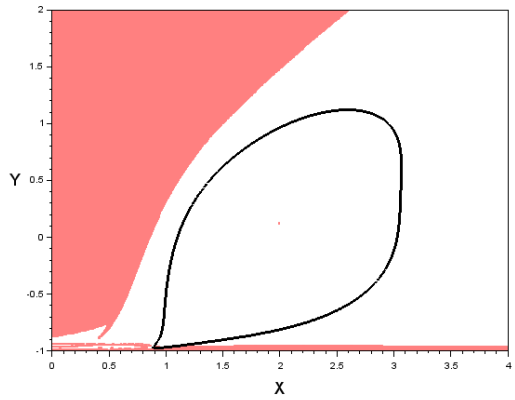

Fig. 28 Level-set of the Lyapunov function computed for the genetic toggle switch (12) with parameters $\alpha_X = 2$, $\alpha_Y = 4$, $\beta = 3$, and $\gamma = 5$ and using formula (13). The area where the orbital derivative is not negative is drawn in red. Since the level-set does not intersect the area where the orbital derivative is nonnegative it is a lower bound on the basin of attraction of the equilibrium at $\mathbf{z} = (0.99634897, 0.12229057)^T$.

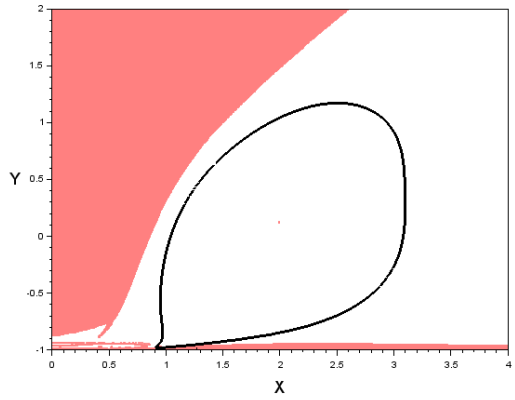

Fig. 29 Level-set of the Lyapunov function computed for the genetic toggle switch (12) with parameters $\alpha_X = 2$, $\alpha_Y = 4$, $\beta = 3$, and $\gamma = 5$ and using formula (14) with $\delta = 0$ and $p = -0.8$. The area where the orbital derivative is not negative is drawn in red. Since the level-set does not intersect the area where the orbital derivative is nonnegative it is a lower bound on the basin of attraction of the equilibrium at $\mathbf{z} = (0.99634897, 0.12229057)^T$.

general positive definite function of the solution under the integral than in [1]. We compared our method for four systems with the method from [1], the method from [23,21] using rational Lyapunov functions, and the method from [3, 4] using sum-of-squares programming. In three of the four cases our method delivered considerably larger inner estimates of the basins of attraction and in the forth there was a tie between our method and [3,4]. We further did a case study for a model of a genetic toggle switch and demonstrated that by using our method one can gain valuable insight into the dynamics of this important model with applications is cybergenetics in a fast and mechanical way.

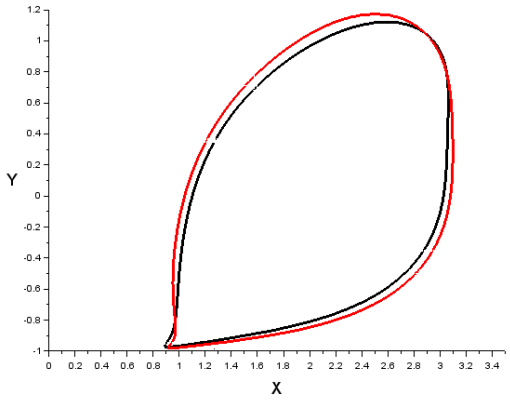

Fig. 30 Comparison of the level-sets of the Lyapunov functions computed for the genetic toggle switch (12) with parameters $\alpha_X = 2$, $\alpha_Y = 4$, $\beta = 3$, and $\gamma = 5$ for the equilibrium at $\mathbf{z} = (0.99634897, 0.12229057)^T$ and using formulas (13) and (14) with $\delta = 0$ and $p = -0.8$. Note that the union of two rigid lower bounds on the basin of attraction is a rigid lower bound on the basin of attraction basin of attraction, and of the equilibrium at .

Acknowledgements This work was supported by the Icelandic Research Fund in the project *Algorithms to compute Lyapunov functions* (no. 130677-051). Additionally the authors would like to thank the anonymous reviewers, whose suggestions improved this manuscript considerably.

Conflict of Interest: The authors declare that they have no conflict of interest.

References

1. Björnsson, J., Giesl, P., Hafstein, S., Kellett, C., Li, H.: Computation of continuous and piecewise affine Lyapunov functions by numerical approximations of the Massera construction. In: Proceedings of the CDC, 53rd IEEE Conference on Decision and Control, pp. 5506–5511. Los Angeles (CA), USA (2014)
2. Björnsson, J., Hafstein, S.: Efficient Lyapunov function computation for systems with multiple exponentially stable equilibria. Procedia Computer Science **108**, 655–664 (2017). Proceedings of the International Conference on Computational Science (ICCS), Zurich, Switzerland, 2017.
3. Chesi, G.: Estimating the domain of attraction for non-polynomial systems via LMI optimizations. Automatica **45**, 1536–1541 (2009)
4. Chesi, G.: Domain of Attraction: Analysis and Control via SOS Programming. Springer (2011)
5. Doban, A.: Stability domains computation and stabilization of nonlinear systems: implications for biological systems. PhD thesis: Eindhoven University of Technology (2016)
6. Doban, A., Lazar, M.: Computation of Lyapunov functions for nonlinear differential equations via a Yoshizawa-type construction. IFAC-PapersOnLine **49**(18), 29 – 34 (2016)
7. Doban, A., Lazar, M.: Computation of Lyapunov functions fornonlinear differential equations via a Massera-type construction. IEEE Trans. Automat. Control **63**(5), 1259–1272 (2018)

8. Gardner, T., Cantor, C., Collins, J.: Construction of a genetic toggle switch in Escherichia coli. Nature **403**(6767), 339–342 (2000)
9. Genesio, R., Tartaglia, M., Vicino, A.: On the estimation of asymptotic stability regions: State of the art and new proposals. IEEE Trans. Automat. Control **30**(8), 747–755 (1985)
10. Giesl, P., Hafstein, S.: Revised CPA method to compute Lyapunov functions for nonlinear systems. J. Math. Anal. Appl. **410**, 292–306 (2014)
11. Giesl, P., Hafstein, S.: Computation and verification of Lyapunov functions. SIAM Journal on Applied Dynamical Systems **14**(4), 1663–1698 (2015)
12. Giesl, P., Hafstein, S.: Review of computational methods for Lyapunov functions. Discrete Contin. Dyn. Syst. Ser. B **20**(8), 2291–2331 (2015)
13. Hachicho, O., Tibken, B.: Estimating domains of attraction of a class of nonlinear dynamical systems with LMI methods based on the theory of moments. In: Proceedings of the 41th IEEE Conference on Decision and Control (CDC), pp. 3150–3155. Los Angeles (CA), USA (2002)
14. Hafstein, S.: A constructive converse Lyapunov theorem on exponential stability. Discrete Contin. Dyn. Syst. **10**(3), 657–678 (2004)
15. Hafstein, S., Kellett, C., Li, H.: Computing continuous and piecewise affine Lyapunov functions for nonlinear systems. Journal of Computational Dynamics **2**(2), 227 – 246 (2015)
16. Hafstein, S., Valfells, A.: Study of dynamical systems by fast numerical computation of Lyapunov functions. In: Proceedings of the 14th International Conference on Dynamical Systems: Theory and Applications (DSTA), vol. Mathematical and Numerical Aspects of Dynamical System Analysis, pp. 220–240 (2017)
17. Kellett, C.: Converse Theorems in Lyapunov's Second Method. Discrete Contin. Dyn. Syst. Ser. B **20**(8), 2333–2360 (2015)
18. Khalil, H.: Nonlinear systems, 3. edn. Pear (2002)
19. Lugagne, J., Carrillo, S., Kirch, M., Köhler, A., Batt, G., Hersen, P.: Balancing a genetic toggle switch by real-time feedback control and periodic forcing. Nature Communications **8**, Art. Nr. 1671 (2017)
20. Massera, J.: Contributions to stability theory. Annals of Mathematics **64**, 182–206 (1956). (Erratum. Annals of Mathematics, 68:202, 1958)
21. Matallana, L., Blanco, A., Bandoni, J.: Estimation of domains of attraction: A global optimization approach. Math. Comput. Modelling **52**(3-4), 574–585 (2010)
22. Sastry, S.: Nonlinear Systems: Analysis, Stability, and Control. Springer (1999)
23. Vannelli, A., Vidyasagar, M.: Maximal Lyapunov functions and domains of attraction for autonomous nonlinear systems. Automatica **21**(1), 69–80 (1985)
24. Vidyasagar, M.: Nonlinear System Analysis, 2. edn. Classics in applied mathematics. SIAM (2002)
25. Wang, W., Ruan, S.: Bifurcations in an epidemic model with constant removal rate of infectives. J. Math. Anal. Appl. **291**(1), 775–793 (2004)
26. Yoshizawa, T.: Stability theory by Liapunov's second method. Publications of the Mathematical Society of Japan, No. 9. The Mathematical Society of Japan, Tokyo (1966)